

## Silicon nanomagnetism

N.T. Bagraev, N.A. Dovator, L.E. Klyachkin  

Ioffe Institute, St. Petersburg, Russia

✉ [leonid.klyachkin@gmail.com](mailto:leonid.klyachkin@gmail.com)

**Abstract.** The paper studied the dependence of the magnitude of the magnetic field induced in the contour formed by the edge channels of the silicon nanosandwich structure on the magnitude of the external magnetic field used for pre-magnetization. The measurements were carried out using a fluxgate magnetometer inside a magnetic screen, which ensures the value of the variation in the magnetic field induction no more than 0.1 nT. The experimental results obtained are in good agreement with preliminary estimates that take into account the energy of negative-U dipoles, and thus confirm the defining role of the spin-orbit interaction in quantum transport in the edge channels of the silicon nanosandwich structure. The presence of nanomagnetism in the contour of the edge channels of nanosandwich structures based on the classical semiconductor silicon, which were created using planar technology methods widely used to create processors and various integrated circuits, is demonstrated for the first time.

**Keywords:** silicon nanosandwich; edge channel; magnetic flux quantum; negative-U centers; nanomagnetism

**Acknowledgements.** *The work was financed within the framework of the State assignment on topic 0040-2019-0017 "Interatomic and atomic-molecular interactions in gases and condensed matter; quantum magnetometry and multiphoton laser spectroscopy".*

**Citation:** Bagraev NT, Dovator NA, Klyachkin LE. Silicon nanomagnetism. *Materials Physics and Mechanics*. 2023;51(7): 1-6. DOI: 10.18149/MPM.5172023\_1.

### Introduction

The development and improvement of planar technology in the first decades of the 21st century has led to the creation of high-performance processors with feature sizes of just a few nanometers. Only a few companies in the world have technologies with element sizes below 14 nm: their competition has led to a race to reduce the size of elements and, accordingly, to increase their number per unit area. However, the situation is currently close to saturation for several reasons. First, there are fundamental physical limitations to creating equipment to implement technology with feature sizes smaller than approximately 1 nm. Secondly, high density of elements in the processor chip, with any variant of its classical architecture (stabilized DC power supply), leads to the flow of a large operating current through a unit area, which requires solving the complex problem of Joule heat removal. The fact that this problem will arise sooner or later became obvious several decades ago. Today it is clear that a further increase in the concentration of elements with a decrease in their size becomes practically impossible.

The search for a solution to this problem has led to the development of a number of alternative directions. One of them is the creation of nanomagnetic chips that perform logical switching under the influence of a magnetic field, which can significantly reduce the energy load compared to a classical processor [1–6]. One such nanomagnetic chip is a multilayer structure consisting of thousands of layers of nanomagnets that can act as individual logic

elements [7]. Scientists working in this direction believe that the use of such chips creates opportunities for parallelization of calculations, and, in addition, makes it possible to offer functions for dynamically changing the processor architecture, which can be optimized each time to perform a specific task.

In addition, in recent decades, special attention has been paid to the development of such a direction of nanophysics as spintronics, which uses the dynamics of the magnetic moment for the transfer and storage of information, as well as the magnetic properties of materials in computational operations [8–12]. Thus, research in this area led to the development of spin magnetic memory devices with a cell size of less than 10 nm, in which information is encoded and stored not in electron charges, as in conventional electronics, but in their spins [13].

It should be noted that from the point of view of the interaction of the electrical and magnetic properties of materials, it is especially tempting to consider the possibility of obtaining magnetic nanostructures without paramagnetic impurities based on classical semiconductors, for example, silicon, to which methods of planar technology widely used to create processors and integrated circuits for various purposes are applicable.

Therefore, another direction, alternative to those described above, is the creation of low-dimensional silicon nanosandwich structures (SNS), in the edge channels (ECs) of which quantum transport of charge carriers is realized at high, up to room, temperatures. Developments in this direction are based on the achievements of nanophysics and nanotechnology of quantum-sized structures, which display size quantization effects, quantum interference, and enable ballistic transport and single-electron tunneling of charge carriers [14,15]. One of the most important experimental results obtained when studying the effects of quantum spin-dependent transport in the above-mentioned SNS structures is the demonstration of the spin field transistor effect [16], which became possible due to the spin–orbit interaction in the ECs, and, accordingly, the resulting quantum spin interference.

This paper presents the results of experiments to study the behavior of the magnetic moment arising in the EC contour in a SNS structure under the influence of an external magnetic field. These experiments are a continuation of studies of spin-dependent transport in SNS structures with the aim of creating SNS-based memory cells that can be switched by a magnetic field.

## Method

An experimental SNS built in Hall geometry, which is an ultra-narrow p-type silicon quantum well (QW) limited by  $\delta$ -barriers heavily doped with boron ( $5 \times 10^{21} \text{ cm}^{-3}$ ) on the surface of n-silicon (100), is shown in Fig. 1(a). It was previously established that edge channels (ECs) are formed in the SNS quantum well during technological processes, and boron atoms in the  $\delta$ -barriers limiting the ECs form trigonal dipole negative-U centers (Fig. 1(b)). This circumstance significantly suppresses electron–electron interaction in such an EC, thus resulting in a long relaxation time of the carriers [15].

It was shown that the EC of the studied SNS consists of pixels: areas of interference of single carriers, and, taking into account the value of their two-dimensional density ( $3 \times 10^{13} \text{ m}^{-2}$ ), the pixel length is approximately 16.1 nm (Fig. 1(c)), and the resistance of a single carrier per pixel is quantized and amounts to " $h/e^2$ ". In this case, each pixel consists of layers containing boron dipoles with an area  $S_{\text{pixel}} = 16.1 \text{ } \mu\text{m} \times 2 \text{ nm}$ , through which the carrier tunnels, since the QW is limited by these two layers with a width and height of approximately 2 nm [17]. In addition, the spin polarization of single carriers was experimentally discovered in the ECs of the SNS under study, and it was concluded that the ECs are coupled and the carriers in them have opposite spin orientations (Fig. 1(d)) [18].

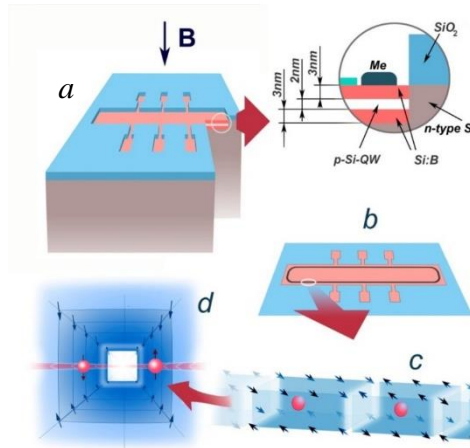


**Fig. 1.** Experimental SNS built in Hall geometry (a); topological edge channel of SNS (b), in which single charge carriers occupy its individual areas, pixels (c); polarized carriers are transported along opposite walls of the edge channel pixels (d)

It was discovered [17] that when varying the magnitude of the magnetic field  $B$  applied perpendicular to the SNS surface, due to Faraday electromagnetic induction, sequential capture of single magnetic flux quanta occurs on single carriers in pixels, and an induction current  $I_{ind}$  appears in the EC:

$$I_{ind} = n \frac{\Delta E}{\Delta \Phi}, \quad (1)$$

where  $\Delta E$  is the change in energy when varying the magnitude of the magnetic flux in the quantum interference region;  $\Delta \Phi = \Delta BS$ ;  $\Delta B$  is the change in the external magnetic field inside the quantum interference region of area  $S$ ;  $n$  is the number of pixels. Previously conducted studies of the de Haas–van Alphen and quantum Hall effects [15] showed that with the above two-dimensional carrier concentration and pixel size, the capture of a magnetic flux quantum by a single pixel occurs at a value of  $\Delta B = 120$  mT. Wherein  $\Delta \Phi = \Delta BS = \Phi_0 = h/e$ . An important factor for further research is that the EC in the SNS is a contour with a length of 4.7 mm and a width of 0.2 mm (Fig. 1(b)).

If the SNS is not connected to any external power source, then, accordingly, no current can flow in its EC other than  $I_{ind}$  induced in the EC pixels by an external magnetic field directed perpendicular to the SNS surface. Moreover, in the case of a high relaxation time in the EC, such an induced current turns out to be persistent [19].

Considering the above, it becomes clear that nanomagnetism can be realized in ECs of SNS structures. Therefore, the purpose of this work was to conduct experiments demonstrating this possibility, namely, to study the induced magnetic field arising in the ECs of a SNS under the influence of an external magnetic field.

The experiments were carried out according to the following procedure. First, the experimental sample at room temperature was placed for 300 seconds in the gap of an electromagnet, which, when turned on, created a homogeneous magnetic field directed perpendicular to the surface of the sample. After this, the sample was removed from the electromagnet gap and placed in a laboratory setup to measure the magnetic moment, at room temperature as well. Then this cycle was repeated multiple times at other values of the external magnetic field.

The laboratory shielded installation used in the experiments is made in the form of a five-layer cylindrical magnetic shield. Moreover, all the internal cylinders are made of M-79 grade permalloy, and the outer cylinder (50 cm in diameter and 70 cm in length) is made of ARMCO steel. The cylinders have lids made of the same material. The innermost cylinder houses a Helmholtz coil powered by a constant (regulated) current supply, which is used both to create an internal uniform magnetic field and to compensate for the residual magnetic field caused by

the penetration (inside the screen) of the external laboratory field and the residual magnetization of permalloys shells. The resulting shielding coefficients (in the frequency range 0–1 Hz) had values of 700 for the longitudinal (along the screen axis) and 5000 for the transverse (perpendicular to the screen axis) components of the magnetic field. During the experiments, the magnitude of variations in the magnetic field induction inside the installation was monitored using a cesium vapor quantum magnetometer and practically did not exceed  $\pm 0.1$  nT.

To measure magnetization (magnetic moment), we used a single-component fluxgate magnetometer with a resolution of  $\sim 0.5$  nT in the frequency band 0–1 Hz. Measurements of the magnetization arising in the sample were carried out as follows. The fluxgate magnetometer placed in the center of the Helmholtz coil was continuously measuring the longitudinal component of the magnetic field of a given value of +30 nT. Then, we moved the (pre-magnetized) sample close to it and measured the shift in the magnitude of the longitudinal component of the magnetic field. The results obtained were used to determine the dependence of the shift in the magnitude of the magnetic field at the location of the fluxgate on the magnitude of the magnetic field of the electromagnet pre-magnetizing the sample.

## Results and Discussion

Figure 2 shows the experimental dependence of magnetization  $M$  arising in the contour formed by the SNS ECs on the external magnetic field of the magnetization performed.

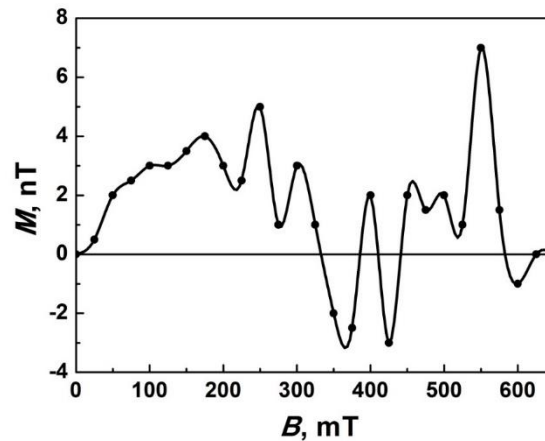


**Fig. 2.** Dependence of the magnetization arising in the contour formed by the SNS ECs on the external magnetic field of the magnetization performed

It was experimentally discovered that the obtained values of  $M$  are maintained for a long time (at least a day), since the current induced by an external magnetic field in the EC contour does not decay in time, due to the fact that transport in the ECs is ballistic in nature. Local maxima in the dependence  $M = f(B)$  correspond to those values of the magnetizing field at which a magnetic flux quantum per pixel is captured (120 mT), i.e. when:

$$\Delta\Phi = \Delta BS = \Phi_0 = h/e \quad (2)$$

However, the experimentally obtained  $B_{\text{ind}}$  values slightly exceed the expected result. Since the magnitude of the energy change when capturing a magnetic flux quantum per pixel  $\Delta E = 2\mu_B\Delta B$  (where  $\mu_B$  is the Bohr magneton), then, taking into account the number of pixels in the EC contour (in the geometry of the experimental sample, the EC length is 9.8 mm; with the above two-dimensional density of single carriers in the EC, the pixel length is 16.1  $\mu\text{m}$ ; number of pixels is 609) and Eq. (2), the expected value of the induced current according to Eq. (1) turns out to be  $I_{\text{ind}} \sim 10^{-10}$  A, which (with the area of the EC contour  $\Delta S = 10^{-6}$  m<sup>2</sup>) is too small to correspond to the obtained experimental results.

This discrepancy between the experimental results and the expected results is explained by the peculiarity of the ECs in the SNS, which is formed between the chains of negative-U boron dipoles. Quantum transport in an EC is carried out along its boundaries by decoupling/coupling of dipoles [20–22]. This means that in the absence of external energy sources and at  $B = 0$ , there are no free carriers in the EC pixels, since they are localized on negative-U dipoles. In this case, since, as was shown in [18], the spin–orbit interaction plays the main role in quantum transport in ECs in SNSs, energy  $E = 44$  meV is required for carrier release. With this value of  $E$  and at  $\Phi \approx \Phi_0 = 4 \cdot 10^{-15}$  Wb,  $n = 609$ , an induced current  $I_{\text{ind}} \approx 2$  mA appears in the EC contour (see (1)). In accordance with Faraday’s law of electromagnetic induction, such a current in the EC limiting the SNS creates a magnetic moment  $P$ , the values of which correspond to the observed value of the measured magnetization  $M$ :

$$M = I_{\text{ind}} S, \quad (3)$$

where  $S \approx 10^{-6}$  m<sup>2</sup> – the area of the EC contour in the model of the frame with the current formed by the SNS limited by the ECs. In this case, the induced current flows through the ECs.

Thus, the obtained experimental values of  $M$  are in good agreement with preliminary estimates that take into account the energy of negative-U dipoles, and, thereby, confirm the decisive role of the spin–orbit interaction in quantum transport in ECs in the SNS. In this case, carriers with both spin up and spin down are induced in the ECs, which make a total contribution to the induced current in the EC contour.

When the external magnetizing field increases to a value corresponding to the capture of a magnetic flux quantum ( $B = 120$  mT), an increase in the value of  $M$  is observed (Fig. 2). The external magnetic field the SNS is placed in of such a magnitude generates a stable induced magnetic field that does not decay for a long time (at least a day). Therefore, the subsequent introduction of a SNS into an external magnetic field of greater magnitude leads to the appearance of an induced current, which, in turn, induces a magnetic field of the opposite direction in it. This effect, similar to the Meissner effect, manifests itself in the oscillating nature of the dependence  $M = f(B)$  with a further increase in the external magnetizing field.

It should be noted that a significant increase in the oscillation amplitude (Fig. 2) with an increase in the external magnetic field may be associated with the possible capture of several magnetic flux quanta at once by a single pixel [15].

## Conclusions

The obtained experimental results for the first time indicate the presence of nanomagnetism in the contour of the edge channels of nanosandwich structures based on the classical semiconductor, silicon, which were created by means of planar technology methods widely used to create processors and various integrated circuits. The demonstrated effect of changing  $\partial E / \partial \Phi$  value is similar to changing entropy  $\partial E / \partial T$ , since the presence of negative-U centers is a regulator of entropy [20,23,24].

## References

1. Kasatkin SI, Murav’ev AM, Amelichev VV, Kostyuk DV. Spin-logic nanoelements. *Bulletin of the Russian Academy of Sciences: Physics*. 2017;81(8): 1023–1026.
2. Arava H, Derlet PM, Vijayakumar J, Cui J, Bingham NS, Kleibert A, Heyderman LJ. Computational logic with square rings of nanomagnets. *Nanotechnology*. 2018;29(26): 265205.
3. Zhao Y, Jiang K, Li C, Liu Y, Zhu G, Pizzochero M, Kaxiras E, Guan D, Li Y, Zheng H, Liu C, Jia J, Qin M, Zhuang X, Wang S. Quantum nanomagnets in on-surface metal-free porphyrin chains. *Nat. Chem*. 2023;15: 53–60.
4. Blachowicz T, Ehrmann A. New Materials and Effects in Molecular Nanomagnets. *Appl. Sci*. 2021;11(16): 7510.

5. Rana B, Mondal AK, Bandyopadhyay S, Barman A. Applications of nanomagnets as dynamical systems: I. *Nanotechnology*. 2022;33(6): 062007.
6. Rana B, Mondal AK, Bandyopadhyay S, Barman A. Applications of nanomagnets as dynamical systems: II. *Nanotechnology*. 2022;33(8): 082002.
7. Becherer M, Breitzkreutz-v. Gamm S, Eichwald I, Ziemys G, Kiermaier J, Csaba G, Schmitt-Landsiedel D. A monolithic 3D integrated nanomagnetic co-processing unit. *Solid-State Electronics*. 2016;115(B): 74–80.
8. Bader SD, Parkin SSP. Spintronics. *Ann. Rev. Condens. Matter. Phys.* 2010;1: 71–88.
9. Csaba G, Imre A, Bernstein GH, Porod W, Metlushko V. Nanocomputing by field-coupled nanomagnets. *IEEE Transactions on Nanotechnology*. 2002;1(4): 209–213.
10. Luo Z, Dao TP, Hrabec A, Vijayakumar J, Kleibert A, Baumgartner M, Kirk E, Cui J, Savchenko T, Krishnaswamy G, Heyderman LJ, Gambardella P. Chirally coupled nanomagnets. *Science*. 2019;363(6434): 1435–1439.
11. Moreno LE, Baldoví JJ, Gaita-Ariño A, Coronado E. Spin states, vibrations and spin relaxation in molecular nanomagnets and spin qubits: a critical perspective. *Chem. Sci.* 2018;9(13): 3265–3275.
12. Chiesa A, Macaluso E, Petiziol F, Wimberger S, Santini P, Carretta S. Molecular Nanomagnets as Qubits with Embedded Quantum-Error Correction. *J. Phys. Chem. Lett.* 2020;11(20): 8610–8615.
13. Hong J, Dong K, Bokor J, You L. Self-assembled single-digit nanometer memory cells. *Applied Physics Letters*. 2018;113(6): 062404.
14. Bagraev NT, Galkin NG, Gehlhoff W, Klyachkin LE, Malyarenko AM. Phase and amplitude response of the '0.7 feature' caused by holes in silicon one-dimensional wires and rings. *J. Phys.: Condens. Matter*. 2008;20(16): 164202.
15. Bagraev NT, Grigoryev VY, Klyachkin LE, Malyarenko AM, Mashkov VA, Rul NI. High-temperature quantum kinetic effect in silicon nanosandwiches. *Low Temperature Physics*. 2017;43(1): 110–119.
16. Klyachkin LE, Bagraev NT, Malyarenko AM. Spin transistor effect in edge channels of silicon nanosandwiches. *Materials Physics and Mechanics*. 2023;51(4): 85-95.
17. Klyachkin LE, Bagraev NT, Malyarenko AM. Macroscopic quantum effects of electromagnetic induction in silicon nanostructures. *Mater. Phys. Mech.* 2022;50(2): 252–265.
18. Bagraev NT, Danilovskii EY, Klyachkin LE, Malyarenko AM, Mashkov VA. Spin Interference of Holes in Silicon Nanosandwiches. *Semiconductors*. 2012;46(1): 75–86.
19. Imri Y. *Introduction to Mesoscopic Physics*. 2002.
20. Bagraev NT, Gusarov AI, Mashkov VA. Spin-correlated transfer of electrons through dangling bonds in semiconductors. *Sov. Phys. JETP*. 1989;68(4): 816–825.
21. Šimánek E. Superconductivity at disordered interfaces. *Solid State Commun.* 1979;32(9): 731–734.
22. Ting CS, Talwar DN, Ngai KL. Possible mechanism of superconductivity in metal-semiconductor eutectic alloys. *Phys. Rev. Lett.* 1980;45(14): 1213–1217.
23. Landauer R. Spatial Variation of Currents and Fields Due to Localized Scatterers in Metallic Conduction. *IBM Journal of Research and Development*. 1957;1(3): 223–231.
24. Landauer R. Electrical resistance of disordered one-dimensional lattices. *The Philosophical Magazine: A Journal of Theoretical Experimental and Applied Physics*. 1970;21(172): 863–867.

## THE AUTHORS

**Bagraev N.T.**

e-mail: bagraev@mail.ioffe.ru

**Dovator N.A.**

e-mail: Nicolai.Dovator@mail.ioffe.ru

**Klyachkin L.E.** 

e-mail: leonid.klyachkin@gmail.com